Available online at www.sciencedirect.com
SCIENCE DIRECT®
Journal of Sound and Vibration 279 (2005) 601–618
JOURNAL OF SOUND AND VIBRATION
www.elsevier.com/locate/jsvi

Vibration analysis of a thin circular plate influenced by liquid/gas interaction in a cylindrical cavity

D.G. Gorman[a,*], C.K. Lee[a], J.M. Reese[a], J. Horáček[b]

[a] *Department of Mechanical Engineering, University of Strathclyde, James Weir Building, Montrose Street, Glasgow G1 1XJ, UK*

[b] *Institute of Thermomechanics, Academy of Sciences of the Czech Republic, Dolejskova 5, 182 00 Prague 8, Czech Republic*

Received 17 February 2003; accepted 11 November 2003

Abstract

This paper describes the free vibration analysis of a cylindrical gas cavity axially bounded at one end by a liquid interface and a thin elastic disc at the other end. Natural frequencies of the complete liquid/gas/structural coupled system are calculated and compared with values obtained when simplifying assumptions are made with respect to the boundaries between the liquid, gas and structure. The analysis includes examination of the interaction between liquid and gas when the disc is assumed rigid. In selected cases the natural frequencies are compared with corresponding values obtained experimentally and from a commercial finite element code.

1. Introduction

The influence of a liquid, or gas, interface upon the higher frequency vibration of a light flexible structure has been a subject of growing interest, particularly due to the increased deployment of thin-walled liquid/gas containers such as pipes and storage vessels. In the literature this work comes under two main headings; structural/acoustic vibration interaction and structural/fluid vibration interaction. In the former the research is confined to the interaction between a light structure and sound pressure waves in an acoustic cavity which the structure is enclosing. The general analysis of acoustic/structural vibration interaction problems is presented in Refs. [1,2], where infinite series solutions for the acoustic pressure and the displacement of the structure are

*Corresponding author.
E-mail address: d.gorman@mecheng.strath.ac.uk (D.G. Gorman).

0022-460X/$ - see front matter © 2004 Elsevier Ltd. All rights reserved.
doi:10.1016/j.jsv.2003.11.052

derived from a fundamental solution of the uncoupled problems, viz.: vibration of the structure in vacuo, and acoustic resonance in a closed cavity with undeformable walls. These basic models were extended and applied to problems involving rectangular plates backed by rectangular cavities [3–6]. One study has been performed on the case of a *circular membrane* vibrating in contact with a gas contained in both a closed and open cylindrical cavity [7]. With respect to the case of vibro-acoustic effects involving a *circular plate*, Lee and Singh [8] analyzed the characteristics of the acoustic radiation emitted from a vibrating circular plate in free space and Gorman et al. [9] considered the case of a circular disc covering a cylindrical acoustic cavity. With respect to structural/fluid vibration interaction in storage containers, Bauer and Chiba [10] considered the case of a circular plate backed by a cylindrical cavity containing fluid assumed to be *viscous and incompressible* and Amabili et al. considered the effect of incompressible liquid depth and contact upon the free vibration of circular and annular plates [11,12].

In this paper an analysis of a particular problem involving gas/liquid/structural interaction is presented. Consider the cylindrical gas cavity shown in Fig. 1 that is encapsulated by the thin circular plate and the liquid column as shown. In this instance the liquid will be assumed to be compressible. This system can be likened to an enclosed and partially filled vertical liquid storage container subject to vertical base vibration excitation. Since the excitation is in the vertical

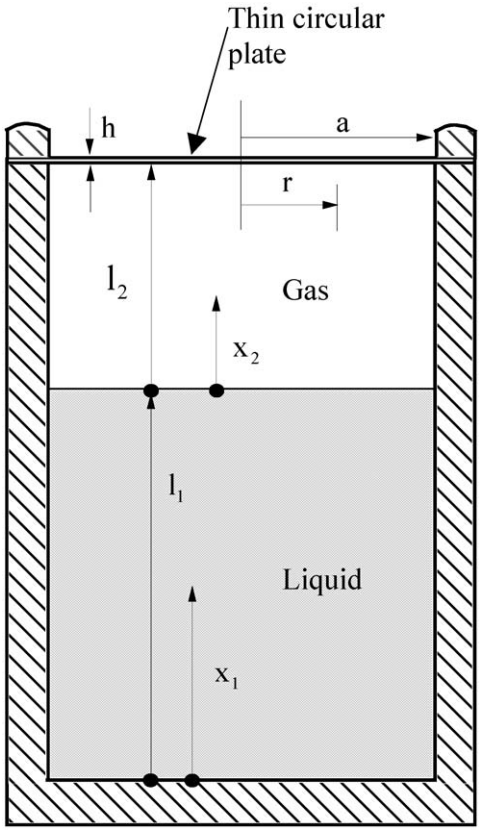

Fig. 1. Schematic diagram of the system under investigation.

direction only, it can reasonably be assumed that the axial stiffness of the side walls is exceptionally high and therefore the only elastic vibration of the structure which need be considered is the thin top plate. When confronted with such a system, the engineer often will seek simplifying assumptions and may in this case make assumptions regarding the liquid/gas and the gas/plate interfaces. In particular, it could well be assumed that either or both, of these interfaces represent solid boundaries whereupon the axial velocity of the gas is zero at all points along these boundary interfaces. In this paper, will be developed a theory upon which the natural frequencies of the completely coupled system can be calculated and the analysis, in passing, will also consider the special case where the rigidity of the plate is so large that it can be considered to be a solid boundary. The results from the analysis are compared with the corresponding values obtained from basic laboratory experiments and from the commercial finite element code ANSYS[1] version 6.1.

2. Theoretical analysis

2.1. Vibration of a cylindrical acoustic medium

Consider the systems shown in Fig. 1 comprising two fluids contained in a solid cylindrical cavity covered by a thin elastic circular plate. For each of the two compressible fluids contained in the cavity ($i = 1$ and 2) the general equation which describes the perturbed velocity potential can be written as

$$\frac{\partial^2 \Phi_i}{\partial \bar{r}^2} + \frac{1}{\bar{r}}\frac{\partial \Phi_i}{\partial \bar{r}} + \frac{1}{\bar{r}^2}\frac{\partial^2 \Phi_i}{\partial \Theta^2} + \left(\frac{a}{l_i}\right)^2 \frac{\partial^2 \Phi_i}{\partial \bar{x}_i^2} = \frac{a^2}{c_i^2}\frac{\partial^2 \Phi_i}{\partial t^2}, \tag{1}$$

where $\bar{r} = r/a$ and $\bar{x}_i = x_i/l_i$ and all symbols are listed in the appendix.

In each case, the harmonic solution can be assumed to be

$$\Phi_i = H_i(\bar{x}_i)Q(\bar{r})\cos(m\Theta)\,\mathrm{e}^{\mathrm{j}\omega t}, \tag{2}$$

where $m = 0, 1, 2$, etc.

Separation of variables yields

$$\left(\frac{a}{l_i}\right)^2 \frac{H_i''}{H_i} = \left(\frac{m^2}{\bar{r}^2} - \lambda_i^2\right) - \left(\frac{Q''}{Q} + \frac{1}{r}\frac{Q'}{Q}\right) \equiv \pm k_i^2, \tag{3}$$

where $\lambda_i = \omega a/c_i$,

$$H_i'' = \frac{\mathrm{d}^2 H_i}{\mathrm{d}\bar{x}_i^2}, \quad Q'' = \frac{\mathrm{d}^2 Q}{\mathrm{d}\bar{r}^2} \quad \text{and} \quad Q' = \frac{\mathrm{d}Q}{\mathrm{d}\bar{r}}.$$

From the Bessel equation (3) with the right-hand side taken equal to $-k_i^2$

$$Q'' + \frac{1}{\bar{r}}Q' + \left[(\lambda_i^2 - k_i^2) - \frac{m^2}{\bar{r}^2}\right]Q = 0 \tag{4}$$

[1] ANSYS is a product of Swanson Analysis Systems, Inc.

and since $\mathrm{d}Q/\mathrm{d}\bar{r}|_{\bar{r}=1} = 0$, for both fluids,

$$Q(\bar{r}) = CJ_m(\alpha_{mq}\bar{r}), \tag{5}$$

where

$$k_{imq}^2 = \{\lambda_i^2 - \alpha_{mq}^2\} \tag{6}$$

and α_{mq} is the qth root of α satisfying $J'_m(\alpha) = 0$.

Considering once again, from Eq. (3), with k_i changing to k_{imq}

$$\left(\frac{a}{l_i}\right)^2 \frac{H_i''}{H_i} = -k_{imq}^2$$

yields

$$H_i(\bar{x}_i) = A_{imq}\cos\gamma_{imq}\bar{x}_i + B_{imq}\sin\gamma_{imq}\bar{x}_i, \tag{7}$$

where $\gamma_{imq} = (l_i/a)k_{imq}$.

For fluid $i = 1$ (liquid), since $\mathrm{d}H_1/\mathrm{d}\bar{x}_1|_{\bar{x}_1=0} = 0$, then

$$\Phi_{1mq} = A_{1mq}[\cos(\gamma_{1mq}\bar{x}_i)]J_m(\alpha_{mq}\bar{r})\cos m\Theta \mathrm{e}^{\mathrm{j}\omega t} \tag{8}$$

and

$$\Phi_1 = \sum_{m=0}^{\infty}\sum_{q=1}^{\infty}\Phi_{1mq} \tag{9}$$

and for the fluid $i = 2$ (gas),

$$\Phi_{2mq} = [A_{2mq}\cos(\gamma_{2mq}\bar{x}_2) + B_{2mq}\sin(\gamma_{2mq}\bar{x}_2)]J_m(\alpha_{mq}\bar{r})\cos(m\theta)\mathrm{e}^{\mathrm{j}\omega t}, \tag{10}$$

$$\Phi_2 = \sum_{m=0}^{\infty}\sum_{q=1}^{\infty}\Phi_{2mq}. \tag{11}$$

Now at the interface between the two fluids, both lateral velocity and pressure must be equal. Hence

$$\frac{1}{l_1}\frac{\partial\Phi_1}{\partial\bar{x}_1}\bigg|_{\bar{x}_1=1} = \frac{1}{l_2}\frac{\partial\Phi_2}{\partial\bar{x}_2}\bigg|_{\bar{x}_2=0} \tag{12}$$

yields

$$B_{2mq} = -\frac{l_2}{l_1}\frac{\gamma_{1mq}}{\gamma_{2mq}}\sin(\gamma_{1mq})A_{1mq}; \tag{13}$$

$$-\rho_1\frac{\partial\Phi_1}{\partial t}\bigg|_{\bar{x}_1=1} = -\rho_2\frac{\partial\Phi_2}{\partial t}\bigg|_{\bar{x}_2=0} \tag{14}$$

yields

$$A_{2mq} = \frac{\rho_1}{\rho_2}\cos(\gamma_{1mq})A_{1mq}. \tag{15}$$

In substituting the above in the general equation (10) for Φ_{2mq} gives

$$\Phi_{2mq} = \frac{l_2}{l_1} A_{1mq} \left[M \cos(\gamma_{1mq}) \cos(\gamma_{2mq}\bar{x}_2) - \left(\frac{\gamma_{1mq}}{\gamma_{2mq}}\right) \sin(\gamma_{1mq}) \sin(\gamma_{2mq}\bar{x}_2) \right] \times J_m(\alpha_{mq}\bar{r}) \cos(m\Theta) e^{j\omega t}, \tag{16}$$

where $M = \rho_1 l_1/(\rho_2 l_2)$.

At this stage, it is convenient to diversify slightly and consider the special case where the assumption, for later comparison, is that the thin plate at $\bar{x}_2 = 1$ is treated as a solid boundary. In this case $\partial\Phi_{2mq}/\partial\bar{x}_2|_{\bar{x}_2=1} = 0$, giving

$$M \tan\gamma_{2mq} + \frac{\gamma_{1mq}}{\gamma_{2mq}} \tan\gamma_{1mq} = 0. \tag{17}$$

From Eq. (17) iteration gives the values of ω contained in the equations for γ_{1mq} and γ_{2mq} which satisfy Eq. (17). However, the gas/structural coupled system will now be analysed by considering in the first instance the free vibration of the thin disc in vacuo.

2.2. Vibration of a thin disc in vacuo

The governing equation for the lateral vibration, $w = w(\bar{r}, \theta, t)$ of a thin disc in vacuo is [13]

$$\left(\frac{\partial^2}{\partial\bar{r}^2} + \frac{1}{\bar{r}}\frac{\partial}{\partial\bar{r}} + \frac{1}{\bar{r}^2}\frac{\partial^2}{\partial\Theta^2}\right)^2 w = -\left(\frac{\rho_d a^4}{D_o}\right)\frac{\partial^2 w}{\partial t^2}, \tag{18}$$

where $D_o = Eh^2/[12(1-\nu^2)]$. For a peripherally-clamped circular plate

$$w|_{\bar{r}=1} = \left.\frac{\partial w}{\partial\bar{r}}\right|_{\bar{r}=1} = 0 \tag{19}$$

and, for a given value of m, the radial mode shape of vibration is

$$W_m(\bar{r}) = A_m J_m(\xi_{ms}\bar{r}) + C_m I_m(\xi_{ms}\bar{r}), \tag{20}$$

where $\xi_{m,s}$ are roots ($s = 1, 2, \ldots$) of the equation

$$J_m(\xi_{ms}) I'_m(\xi_{ms}) - I_m(\xi_{ms}) J'(\xi_{ms}) = 0. \tag{21}$$

The natural frequencies of the disc in vacuo are

$$\omega_{ms} = \xi_{ms}^2 \frac{1}{a^2}\sqrt{\frac{D_o}{\rho_d}} \tag{22}$$

and the modes of vibration are

$$W_{ms}(\bar{r}) = -\frac{I_m(\xi_{ms})}{J_m(\xi_{ms})} J_m(\xi_{ms}\bar{r}) + I_m(\xi_{ms}\bar{r}). \tag{23}$$

2.3. The coupled solution

From Eq. (16), for a fixed integer value m (the number of nodal diameters), the potential is

$$\Phi_{2m} = \sum_{q=1}^{+\infty} \frac{l_2}{l_1} A_{1mq} \left[M \cos(\gamma_{1mq}) \cos(\gamma_{2mq}\bar{x}_2) - \left(\frac{\gamma_{1mq}}{\gamma_{2mq}}\right) \sin(\gamma_{1mq}) \sin(\gamma_{2mq}\bar{x}_2) \right] \times J_m(\alpha_{mq}\bar{r}) \cos(m\Theta) e^{j\omega t} \tag{24}$$

and for the forced vibrations of the disc it is possible to write

$$w_m(\bar{r}, \Theta, t) = W_m(\bar{r}) \cos(m\Theta) e^{j\omega t}, \tag{25}$$

where

$$W_m(\bar{r}) = \sum_{s=1}^{+\infty} W_{0ms}\, W_{ms}(\bar{r}) \tag{26}$$

and W_{0ms} are unknown constants. Now equating the velocity of the plate to the axial velocity of the gas at the structural/gas interface:

$$\frac{1}{l_2} \frac{\partial \phi_{2m}}{\partial \bar{x}_2}\bigg|_{\bar{x}_2=1} = \frac{\partial w_m}{\partial t} \tag{27}$$

yields

$$-\sum_{q=1}^{+\infty} \frac{l_2}{l_1} A_{1mq} [M\gamma_{2mq} \cos(\gamma_{1mq}) \sin(\gamma_{2mq}) + \gamma_{1mq} \sin(\gamma_{1mq}) \cos(\gamma_{2mq})]\, J_m(\alpha_{mq}\bar{r}) = j\omega l_2\, W_m(\bar{r}). \tag{28}$$

At this stage the orthogonality relationship [14] is also introduced:

$$\int_0^1 \bar{r} J_m(\alpha_{mq_1}\bar{r}) J_m(\alpha_{mq_2}\bar{r})\, d\bar{r} = 0 \tag{29}$$

for $q_1 \neq q_2$. For $q_1 = q_2 = q$,

$$\int_0^1 \bar{r} J_m^2(\alpha_{mq}\,\bar{r})\, d\bar{r} = \frac{1}{2}\left(1 - \frac{m^2}{\alpha_{mq}^2}\right) J_m^2(\alpha_{mq}). \tag{30}$$

Therefore, multiplication of Eq. (28), which describes the impermeability condition, by $[\bar{r}J_m(\alpha_{mq}\bar{r})]$ and integration over the interval (0,1) gives

$$\frac{l_2}{l_1} A_{1mq} = \frac{-j\omega l_2 \int_0^1 \bar{r} W(\bar{r}) J_m(\alpha_{mq}\bar{r})\, d\bar{r}}{\gamma_{2mq}[M \cos(\gamma_{1mq}) \sin(\gamma_{2mq}) + (\gamma_{1mq}/\gamma_{2mq}) \sin(\gamma_{1mq}) \cos(\gamma_{2mq})] J_m^2(\alpha_{mq}) \frac{1}{2}(1 - m^2/\alpha_{mq}^2)}. \tag{31}$$

Therefore,

$$\phi_{2m}|_{\bar{x}_2=1} = \mathrm{j}\omega l_2 \sum_{q=1}^{+\infty} K_{12mq}^{(\omega)} \frac{J_m(\alpha_{mq}\bar{r})}{\frac{1}{2}(1-(m^2/\alpha_{mq}^2))J_m^2(\alpha_{mq})} \cos(m\Theta)\mathrm{e}^{\mathrm{i}\omega t} \times \int_0^1 \bar{r} W_m(\bar{r}) J_m(\alpha_{mq}\bar{r})\,\mathrm{d}\bar{r}, \tag{32}$$

where

$$K_{12mq}^{(\omega)} = \frac{-[M\cos(\gamma_{1mq})\cos(\gamma_{2mq}) - (\gamma_{1mq}/\gamma_{2mq})\sin(\gamma_{1mq})\sin(\gamma_{2mq})]}{\gamma_{2mq}[M\cos(\gamma_{1mq})\sin(\gamma_{2mq}) + (\gamma_{1mq}/\gamma_{2mq})\sin(\gamma_{1mq})\cos(\gamma_{2mq})]} \tag{33}$$

and

$$p_m(\bar{r},\Theta,t)|_{\bar{x}_2=1} = -\rho_2 \left.\frac{\partial \phi_{2m}}{\partial t}\right|_{\bar{x}_2=1} = 2\,\rho_2 l_2 \omega^2 \cos(m\Theta)\mathrm{e}^{\mathrm{j}\omega t} \sum_{q=1}^{+\infty} p_{mq}(\bar{r}), \tag{34}$$

where

$$p_{mq}(\bar{r}) = K_{12mq}^{(\omega)} \frac{J_m(\alpha_{mq}\bar{r})}{(1-m^2/\alpha_{mq}^2)\,J_m^2(\alpha_{mq})} \int_0^1 \bar{r} W_m(\bar{r}) J_m(\alpha_{mq}\bar{r})\,\mathrm{d}\bar{r}. \tag{35}$$

Substituting $W_{ms}(\bar{r})$ from Eq. (23) into the integrals $\int_0^1 \bar{r} W_{ms}(\bar{r}) J_m(\alpha_{mq}\bar{r})\,\mathrm{d}\bar{r}$, gives

$$\int_0^1 \bar{r} W_{ms}(\bar{r})\, J_m(\alpha_{mq}\bar{r})\,\mathrm{d}\bar{r} = J_m(\alpha_{mq}) I_m(\xi_{ms}) G_{msq}, \tag{36}$$

where

$$G_{msq} = \left[\frac{\xi_{ms}}{(\alpha_{mq}^2+\xi_{ms}^2)} \frac{I_m'(\xi_{ms})}{I_m(\xi_{ms})} - \frac{\xi_{ms}}{(\alpha_{mq}^2-\xi_{ms}^2)} \frac{J_m'(\xi_{ms})}{J_m(\xi_{ms})}\right]. \tag{37}$$

Therefore, the pressure equation (34) becomes

$$p_m(\bar{r},\Theta,t) = 2(\rho_2 l_2)\omega^2 \cos(m\Theta)\mathrm{e}^{\mathrm{i}\omega t} \sum_{q=1}^{+\infty} K_{12mq}^{(\omega)} \frac{J_m(\alpha_{mq}\bar{r})}{(1-m^2/\alpha_{mq}^2)J_m(\alpha_{mq})} \times \sum_{s=1}^{+\infty} W_{0ms} I_m(\xi_{ms}) G_{msq}. \tag{38}$$

For the disc in vacuo,

$$\nabla^4 W_{ms}(r) = \frac{\rho_d}{D_o}\omega_{ms}^2 W_{ms}(\bar{r}) \tag{39}$$

and the substitutions of

$$w_m(r,\Theta,t) = \cos(m\Theta)\mathrm{e}^{\mathrm{i}\omega t} \sum_{s=1}^{+\infty} W_{0ms} W_{ms}(\bar{r}) \tag{40}$$

and $p_m|_{x_2=1}$ into the equation of motion describing the vibrating disc interacting with the fluid, i.e.,

$$\nabla^4 w = -\frac{\rho_d}{D_o}\frac{\partial^2 w}{\partial t^2} + \frac{p}{D_o h}\bigg|_{\bar{x}_2=1} \tag{41}$$

yields

$$\frac{\rho_d}{D_o}\sum_{s=1}^{+\infty} W_{0,m,s}[\omega_{m,s}^2 - \omega^2]W_{m,s}(\bar{r}) = \frac{p_m}{D_o h}\bigg|_{\bar{x}_2=1}. \tag{42}$$

After substitutions of W_{ms} and p_m,

$$\begin{aligned}\sum_{s=1}^{+\infty}\left(\frac{\rho_d}{D_o}\right)[\omega_{ms}^2 - \omega^2]W_{0ms}\left[-\frac{I_m(\xi_{ms})}{J_m(\xi_{ms})}J_m(\xi_{ms}\bar{r}) + I_m(\xi_{ms}\bar{r})\right]\\ = 2(\rho_2 l_2 D_o h)\omega^2\sum_{s=1}^{+\infty} W_{0ms}I_m(\xi_{ms})\sum_{q=1}^{+\infty} K_{12mq}^{(\omega)}\, G_{msq}\frac{J_m(\alpha_{mq}\bar{r})}{(1 - m^2/\alpha_{mq}^2)J_m(\alpha_{mq})}.\end{aligned} \tag{43}$$

Multiplying Eq. (43) by $[\bar{r}J_m(\alpha_{mq}\bar{r})]$ and integrating over the interval $(0, 1)$, the following equation is obtained:

$$\begin{aligned}\sum_{s=1}^{+\infty}[\omega_{ms}^2 - \omega^2]W_{0ms}\int_0^1 \bar{r}J_m(\alpha_{mp}\bar{r})\left[-\frac{I_m(\xi_{ms})}{J_m(\xi_{ms})}J_m(\xi_{ms}\bar{r}) + I_m(\xi_{ms}\bar{r})\right]\mathrm{d}\bar{r}\\ = 2\rho\,\omega^2\sum_{s=1}^{+\infty} W_{0ms}I_m(\xi_{ms})\sum_{q=1}^{+\infty} K_{12mq}^{(\omega)}G_{msq}\frac{1}{(1 - m^2/\alpha_{mq}^2)J_m(\alpha_{mq})}\\ \times\int_0^1 \bar{r}J_m(\alpha_{mp}\bar{r})\,J_m(\alpha_{mq}\bar{r})\,\mathrm{d}\bar{r},\end{aligned} \tag{44}$$

where $\rho = \rho_2 l_2/(\rho_d h)$. After the integration has been performed, the following equation is obtained:

$$\begin{aligned}\sum_{s=1}^{+\infty}[\omega_{ms}^2 - \omega^2]W_{0ms}I_m(\xi_{ms})G_{msq}J_m(\alpha_{mq})\\ = \rho\omega^2\sum_{s=1}^{+\infty} W_{0ms}I_m(\xi_{ms})K_{12mq}^{(\omega)}G_{msq}J_m(\alpha_{mq})\end{aligned} \tag{45}$$

which, upon rearranging, gives

$$\sum_{s=1}^{+\infty} W_{0ms}I_m(\xi_{ms})\{[\omega_{ms}^2 - \omega^2]G_{msq}J_m(\alpha_{mq}) - \rho\omega^2 K_{12mq}^{(\omega)}\,G_{msq}J_m(\alpha_{mq})\} = 0. \tag{46}$$

Expressing Eq. (46) in matrix form for fixed m and q, $s = 1, 2, \ldots, N$ gives

$$\begin{bmatrix} a_{11}(\omega) & a_{12}(\omega)\cdots & a_{1N}(\omega) \\ a_{21}(\omega) & a_{22}(\omega)\cdots & a_{2N}(\omega) \\ \vdots & \vdots & \vdots \\ \cdots & a_{qs}(\omega) & \cdots \\ \vdots & \vdots & \vdots \\ a_{N1}(\omega) & a_{N2}(\omega)\cdots & a_{NN}(\omega) \end{bmatrix} \begin{bmatrix} \bar{W}_{m,1} \\ \bar{W}_{m,2} \\ \vdots \\ \bar{W}_{m,s} \\ \\ \bar{W}_{m,N} \end{bmatrix} = \begin{bmatrix} 0 \\ 0 \\ \vdots \\ 0 \\ \vdots \\ 0 \end{bmatrix}, \tag{47}$$

where

$$a_{qs}(\omega) = J_m(\alpha_{mq}).G_{msq}.\{\omega_{ms}^2 - \omega^2[1 + \rho K_{12mq}^{(\omega)}]\}, \tag{48}$$

$$\bar{W}_{ms} = W_{0ms} I_m(\xi_{ms}). \tag{49}$$

3. Experimental and ANSYS analysis

3.1. Experimental Analysis

A simple experimental arrangement of the system shown in Fig. 1 was constructed in which a 5 mm thick Perspex tube was fixed upon a shaker table. A microphone inserted into the wall of the tube detects acoustic resonance. A thin circular disc covered the top of the perspex tube and resonance of the disc was detected by a miniature accelerometer. This arrangement will be referred to as the "plate top" case (Fig. 2a). A similar arrangement, except that a solid cap replaced the thin disc thus modelling the condition described by Eq. (17), was tested. In this case two microphones are used to detect acoustic resonance of the air column; one into the side of the Perspex wall as before and the other into the Perspex solid top. This arrangement will be referred to as the "hard-top" case (Fig. 2(b)).

In both cases the heights of water and air columns can be adjusted and since the excitation is whole base vertical excitation, then only the axisymetric ($m = 0$) modes can be excited.

The radius of the liquid and cavity and the circular plate at the top, a, was 65 mm and the thickness of the thin structural circular plate was 0.8 mm. In view of the manner in which the plate was fastened it was assumed that the boundary conditions were predominantly clamped.

3.2. ANSYS analysis

The model was fully three dimensional and used 9000 elements (type FLUID30) for the fluids in the cavity and 300 elements (type SHELL63) for the plate. The Perspex cylinder walls were (a) assumed rigid, and (b) modelled by 3600 elements (type SHELL63) which were attributed values of Young's modulus, density and the Poisson ratio of 4.8 GPa, 1180 kg/m^3 and 0.3, respectively. In each of the cases (a) and (b), the circular plate was fully fixed to the edges of the cylinder wall. The plate and fluid elements that are in contact are coupled for fluid–structure interaction. A modal analysis was performed and the Lanczos unsymmetric eigensolver method [15] was used for

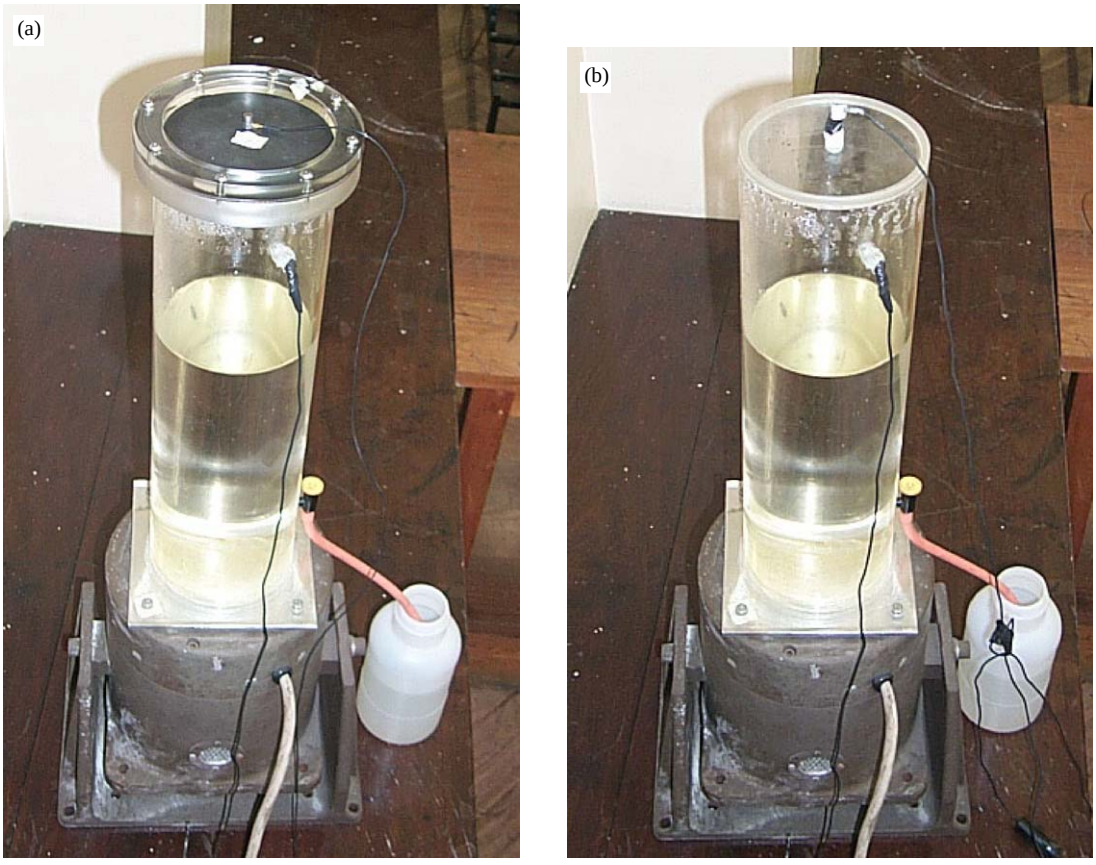

Fig. 2. (a) Experiment involving liquid/gas/structural interaction (“plate top”); (b) Experiment involving liquid/gas interaction only (“hard top”).

the mode extraction during the solution process. The dimensions of the plate and cavity were the same as those in the experiments.

4. Results and discussion

4.1. “Hard top” case

Prior to presenting results for the complete coupled liquid/gas/structure system, the natural frequencies of the liquid/gas cavity were first considered, where the top is assumed solid, as determined from Eq. (17). In accordance with the experimental method of excitation, the results are confined to those associated with axisymetric modes of vibration, i.e., $m = 0$ in Eq. (2). Furthermore, in this case only, only the fundamental mode was considered where there are no radial waves in the liquid or gas, i.e., $s = 1$, rendering $\alpha_{01} = 0$ and hence $Q(\bar{r}) = 1$ in Eq. (2). Now, since $q = 1$, then $\gamma_{101} = \omega l_1/c_1 = \bar{\gamma}_{101}$ for the liquid and $\gamma_{201} = \omega l_2/c_2 = \bar{\gamma}_{201}$ for the gas. In this

special case, for $q = 1$, these parameters are denoted as $\bar{\gamma}_{101}$ and $\bar{\gamma}_{201}$. Accordingly $\bar{\gamma}_{101} = f_{12}\bar{\gamma}_{201}$, where $f_{12}(= l_1/c_1/l_2/c_2)$ is a constant which in effect describes the degree of potential coupling between the liquid and the gas.

Therefore, Eq. (17) can now be written as

$$\tan \bar{\gamma}_{201} + \frac{1}{N} \tan f_{12}\bar{\gamma}_{201} = 0, \tag{50}$$

where $N = \rho_1 c_1/(\rho_2 c_2)$.

Eq. (50) is iterated for values of $\bar{\gamma}_{201}(= \omega l_2/c_2)$ for set values of f_{12} and N. Figs. 3(a) and (b) show plots of the first ($\bar{\gamma}^1_{201}$) and second ($\bar{\gamma}^2_{201}$) root, respectively, of $\bar{\gamma}_{201}$ against f_{12} $(0.1 \leqslant f_{12} \leqslant 2)$ for a value of $N = 3644.3$ ($c_1 = 1500$ m/s, $\rho_1 = 1000$ kg/m^2, $c_2 = 343$ m/c, $\rho_2 = 1.2$ kg/m^3). Figs. 3(a) and (b) show the values of π and 2π, respectively, since these would be the first two roots of $\bar{\gamma}_{201}$ if the liquid/gas interface was assumed rigid. Also included in these figures are the values of $\omega l_2/c_2$ determined experimentally as described in Section 3.

Referring to Figs. 3(a) and 3(b), there would appear to be good agreement between the computed and the experimental values. It is also interesting to note that the first root of $\bar{\gamma}_{201}$ only reaches the value of π for values of f_{12} less than approximately 0.5 with the exception when $f_{12} = 1$. In this case it can immediately be seen that for $f_{12} = 1$, Eq. (50) simply becomes $\tan \bar{\gamma}_{201} = 0$, i.e., $\bar{\gamma}_{201} = \pi, 2\pi$ etc. Likewise for the second root of $\bar{\gamma}_{201}$ (Fig. 3(b)) the value of 2π is only reached for values of f_{12} less than approximately 0.25 with the exception when $f_{12} = 1$ (as before for the first root) and, more interestingly, for $f_{12} = 0.333$ (one third). Due to the very large value of N in Eq. (50), roots such as these will indeed be generated. However, in practice it would be very unlikely for such special roots to manifest themselves due to the absolute accuracy required in all relative dimensions and properties to exist. Outwith these notable exceptions one can deduce that in the case where the disc covering the top of the cavity is assumed solid, then the natural

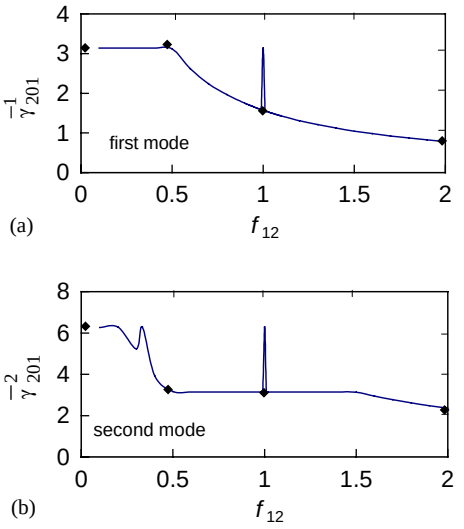

Fig. 3. Values of the first two roots for $\bar{\gamma}_{201}$ against f_{12}.

frequencies of the gas cavity can only be assumed to be similar to the case of a totally solid enclosed gas cavity if the natural frequencies of the liquid column alone are approximately at least twice and four time that of the gas cavity alone for the first and second modes, respectively. If this is not the case then the complete liquid/gas coupled system must be considered.

4.2. "Plate-top" case

In this section the results produced for the case where the top of the container is the thin circular plate will be considered. In this case a fluid/gas/structural interaction system is in effect being examined.

4.2.1. Comparison between experimentally obtained and computed values of natural frequency

For this particular comparison, the authors deemed that the basic construction of the experimental set-up was only suitable for comparison of the fundamental modes of vibration for each height of liquid and gas. The main sources of error between the experimental and computed values no doubt lie in the compliance of the actual boundary conditions with the assumed conditions for the circular plate $[(\partial w/\partial \bar{r}|_{\bar{r}=1} = w|_{\bar{r}=1} = 0)]$, and the compliance of the Perspex cylinder wall. In addition the mass of the, albeit small, accelerometer was not accounted for.

Accordingly, Table 1 lists the values of the fundamental natural frequencies obtained experimentally, those corresponding values obtained by solving for the determinant of the first three rows and columns of the matrix described by Eq. (47) equated to zero, and, those corresponding values obtained from execution of the ANSYS 6.1 model for both the cases where the cylinder wall was assumed rigid and compliant. For reference, also contained in Table 1 are:

(i) The values ω_{d1} and ω_{d2} which are the first two computed axisymetric natural frequency of the disc in vacuo, i.e., from Eq. (22)

$$\omega_{d1} = \zeta_{01}^2 \frac{1}{a^2}\sqrt{\frac{D_o}{\rho_\alpha}} \quad \text{and} \quad \omega_{d2} = \zeta_{02}^2 \frac{1}{a^2}\sqrt{\frac{D_o}{\rho_\alpha}},$$

where in this case for a peripherally clamped disc, $\zeta_{01}^2 = 10.2158$ and $\zeta_{02}^2 = 39.771$.

(ii) Values of ω_{wa1}, ω_{wa2}, ω_{wa3} which are the computed first, second and third natural frequencies of the liquid/gas system only respectively, when the top is assumed rigid, i.e., the "hard-top" case reproduced from Section 4.1, using Eq. (50).

By listing the values described above, it will help the reader to classify the natural frequencies computed from Eq. (47), ANSYS and experimental values for the liquid/gas/structural interaction case. In all cases natural frequencies are expressed in units of Hertz.

From the results shown in Table 1, there would appear to be reasonably good correlation between the values of natural frequencies computed from Eq. (47) and ANSYS, and both show the same basic trend for decreasing values of f_{12}. In the case of the fundamental mode only, the value obtained experimentally is found to be always somewhat lower than the computed values. Accordingly, the analysis by ANSYS was, as previously described, modified to include the effect of the compliance of the Perspex side walls and the corresponding computed fundamental natural frequencies and listed in Table 1; values contained in brackets. Consequently, it is observed that

Table 1
Values of natural frequencies computed and compared with experimentally obtained values. All values of ω expressed in Hertz

l_1 (mm)	l_2 (mm)	ω Eq. (47)	ω (ANSYS)	$\omega_{\text{experimental}}$	ω_{d1} ω_{d2} Eq. (22)	ω_{wa1} ω_{wa2} ω_{wa3} Eq. (50)
400	45	489	486(438)[a]	460	483	938
		938	1053			2812
$f_{12} = 1.98$		1876	1870		1882	3811
		2812	2715			
350	95	484	484(430)	440	483	1071
		1071	1036			1805
$f_{12} = 0.997$		1799[b]	1850		1882	3214
		1883[b]	1892			
300	145	482	482(426)	476	483	1182
		1183	975			1251
$f_{12} = 0.473$		1251	1459		1882	2365
		1875	1870			
200	245	480	480(425)	441	483	700
		703	674			1400
$f_{12} = 0.23$		1400	1322		1882	1875
		1874	1830			
150	295	477	477(420)	445	483	581
		587	574			1163
$f_{12} = 0.11$		1164	1144		1882	1744
		1743	1723			
100	345	467[c]	466(411)	434	483	497
		512[c]	509			994
$f_{12} = 0.066$		998	995		1882	1491
		1492	1517			

[a] Numbers in bracket are those for the system modelled with compliant side walls.
[b] Coupled ω_{d2} and ω_{wa2}.
[c] Coupled ω_{d1} and ω_{wa1}.

the values obtained experimentally always lie between those values computed for a rigid side wall assumption and those computed for a compliant side wall assumption.

The comparison between the values of natural frequency obtained from Eq. (47) and from ANSYS would appear to be good, particularly, for the low fractional values of f_{12}. The same comparison for values of f_{12} between 2 and 0.5, i.e., in and around a value of f_{12} equal to 1 shows less strong agreement particularly for the second mode. In the view of the authors, this less accurate agreement is mainly attributable to one important difference of the two methods. In the analysis presented it is implied that at the interface between the liquid and gas and between the gas and the plate, only axial displacement is compatible, i.e., the boundary is defined as *affined*. However, in the ANSYS formulation these interfaces are linked by complete compatibility in all directions. This difference in modelling of the interfaces will have a more pronounced effect at conditions of strong interaction.

4.2.2. General characteristics of liquid/gas/struction interaction system

Prior to presenting results for more general cases, an attempt shall be made to define and describe parameters which describe degrees of coupling between the liquid gas and structure.

In Section 4.1 the parameter f_{12} was defined as

$$\bar{\gamma}_{101} = f_{12}\bar{\gamma}_{201} \quad \text{or} \quad f_{12} = \frac{l_1/c_1}{l_2/c_2},$$

where $\bar{\gamma}_{101}$ and $\bar{\gamma}_{201}$ are the values of γ_{101} and γ_{201}, respectively, for the special case where $q = 1$. Now, consider the first computed root from Eq. (50), i.e.,

$$\bar{\gamma}^1_{201} = \omega_{wa1}\frac{l_2}{c_2}, \quad \text{hence} \quad \omega_{wa1} = \bar{\gamma}^1_{201}\frac{c_2}{l_2}. \tag{51}$$

The first axisymetric natural frequency of the disc in vacuo, ω_{d1} can be written as

$$\omega_{d1} = \zeta^2_{01}\sqrt{\frac{D_o}{\rho_d a^4}} = \zeta^2_{01}\{\bar{D}\}^{1/2}.$$

Now let the parameter f_{32} be defined as

$$\omega_{d1} = f_{32}\omega_{wa1}.$$

In effect f_{32} is the ratio of the natural frequency of the first axisymetric mode of the disc in vacuo to the first natural frequency of the solid bounded liquid/gas sub-system.

Now in Eq. (48) the eigenvalue ω^2 can be written as

$$\omega^2 = \zeta^4\bar{D}$$

and for the disc in vacuo, as before,

$$\omega^2_{mn} = \zeta^4_{ms}\bar{D}.$$

Hence, Eq. (48) becomes

$$a_{qs}(\zeta) = J_m(\alpha_{mq})G_{msq}\{\zeta^4 - \zeta^4_{ms}[1 + \rho K^{(\zeta)}_{12mq}]\}$$

and the values of γ_{1mq} and γ_{2mq} contained in $K^{(\omega)}_{12mq}$ (Eq. (33)) become

$$\gamma_{1mq} = \sqrt{\frac{\zeta^4}{\zeta^4_{01}}(f_{12}f_{32}\,\bar{\gamma}^1_{201})^2 - \left(\alpha_{mq}f_{12}\frac{c_1}{c_2}\frac{l_2}{a}\right)^2}$$

and

$$\gamma_{2mq} = \sqrt{\frac{\zeta^4}{\zeta^4_{01}}(f_{32}\,\bar{\gamma}^1_{201})^2 - \left(\alpha_{mq}\frac{l_2}{a}\right)^2}.$$

Therefore, the roots of the matrix equation (40), ζ, will depend upon the non-dimensional parameters of f_{12}, f_{32}, $\rho(=\rho_2 l_2/(\rho_d h))$, $M(=\rho_1 l_1/(\rho_2 l_2))$ and (l_2/a). Furthermore, if ρ_1, ρ_2, c_1 and c_2 are specified then specification of f_{12} and f_{32} negate the need to specify ρ and M. Hence f_{12}, f_{32} and the ratio (l_2/a) are the sole governing parameters of the matrix equation (40). Now consider the general case where $(l_2/a) = 0.25$, and as before $\rho_1 = 1000\ \text{kg/m}^3$, $\rho_2 = 1.2\ \text{kg/m}^3$, $c_1 = 1500\ \text{m/s}$ and $c_2 = 343\ \text{m/s}$. The first three rows and columns of matrix equation (40) for roots of

ζ shall be solved for varying values of f_{32} (adjusting the plate thickness relative to l_2) and f_{12} (adjusting the water depth l_1 relative to l_2).

From the experience of Section 4.2a, the main interest here focuses upon the first structural dominant natural frequency and the first liquid/gas dominant natural frequency and strong coupling occurs when these two values approach each other. Therefore, let

$$R_c = \zeta_{d1}/\zeta_{wa1}, \tag{52}$$

where ζ_{d1} and ζ_{wa1} are the first structural dominated and first liquid/gas dominated related roots, respectively, of the truncated matrix equation (47). Therefore, strong liquid/gas/structural coupling will be indicated when R_c approaches unity.

Figs. 4(a)–(d) are plots of R_c against f_{12} for four values of f_{32} between 0.4 and 1.6. From these figures it can be seen that the value of R_c is generally in agreement with the value of f_{32}. The only instances where disagreement occurs is around $f_{12} = 1$ due to the strong coupling between the liquid and gas columns.

Now consider the case where the first natural frequency of the disc in vacuo is tuned relative to the first natural frequency of the gas column alone, i.e., both the disc and liquid interfaces are assumed as rigid boundaries. In this case replacing $\bar{\gamma}^1_{201}$ by π in Eq. (51) gives

$$\omega_{wa1} = \frac{\pi c_2}{l_2}$$

and

$$\omega_{d_1} = \zeta_{01}^2 \sqrt{\frac{D_o}{\rho_d a^4}} = F_{32}\omega_{wa1}.$$

Figs. 5(a)–(d) show plots of R_c against values of f_{12} ranging between 0.1 and 2 for values of F_{32} equal to 0.4, 0.8, 1.2 and 1.6 as before. Comparing Figs. 5(a)–(d) with the corresponding values in

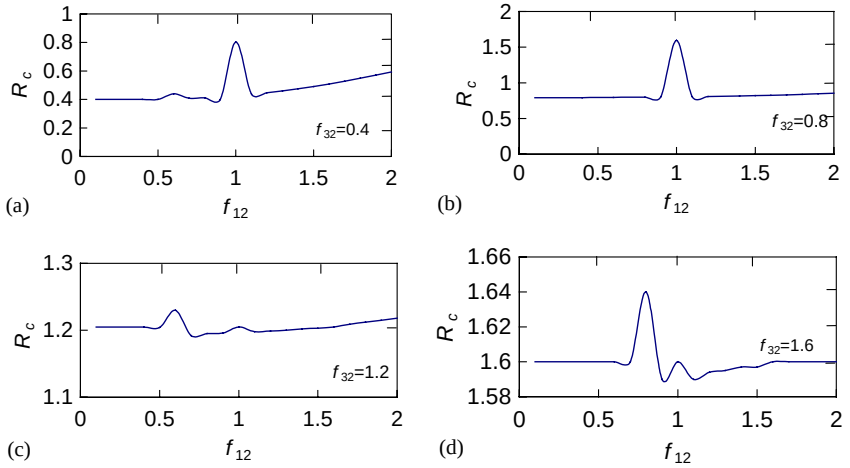

Fig. 4. Plot of R_c versus f_{12} when disc is relatively tuned to liquid/gas acoustic cavity.

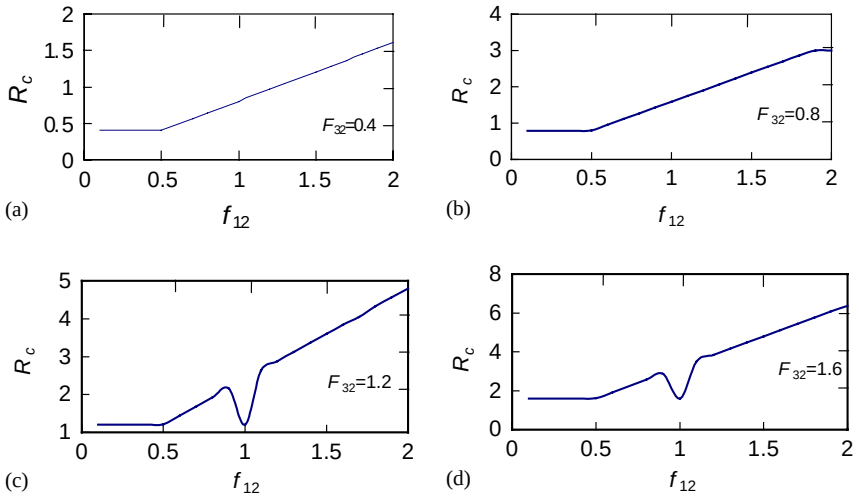

Fig. 5. Plot of R_c versus f_{12} when disc is relatively tuned to gas only acoustic cavity.

Figs. 4(a)–(d), one sees that R_c corresponds approximately to R_c for lower values of f_{12}. However, R_c then increases linearly with increasing values of f_{12}. This is of particular importance in the cases where F_{32} is less that unity, whence in such cases the value of R_c can pass through the value of unity, indicating a condition of strong liquid/gas/structural coupling, a situation that is generally intended to be avoided.

5. Conclusions

An analysis describing the free vibration of a liquid/gas/structural interacting system has been presented. Results from the natural frequency for the coupled system have been produced which compare favourably with values computed from a commercial finite element code and experimentally obtained values. The results for the completely coupled system were also compared with values obtained when simplifying assumptions were made about the liquid/gas and gas/structure interfaces. It was concluded that only under very specific circumstances could these simplifying assumptions render values of the natural frequency that resembled those corresponding values from a complete analysis of the coupled system.

Acknowledgements

The research is supported by the Grant Agency of the Academy of Sciences of the Czech Republic, project No. A2076101/01 (Natural Vibration and Stability of Shells in Interaction with Flowing Fluid) and The Royal Society (London).

Appendix. Nomenclature

a	peripheral radius of disc/acoustic cavity
c_1, c_2	speed of acoustic wave propagation in liquid and gas column, respectively
E	Young's modulus
f_{12}, f_{32}, F_{32}	coupling factors
J_m, I_m, Y_m	Bessel functions, order m
l_1, l_2	depth of liquid and gas cavity, respectively
m	number of circular waves
q	number of radial waves in acoustic medium
r	radial co-ordinate
s	number of radial waves on disc
w	lateral vibratory deflection of disc
x_1, x_2	axial distance from base of liquid and gas cavity, respectively
Θ	circumferential co-ordinate
Φ	velocity potential functions
v	Poisson's ratio
ρ_1, ρ_2	density of liquid and gas, respectively
ρ_d	disc density
ω	natural frequency

References

[1] E.H. Dowell, G.F. Gorman, D.A. Smith, Acoustoelasticity: general theory, acoustic natural modes and forced response to sinusoidal excitation, including comparisons with experiment, *Journal of Sound and Vibration* 52 (4) (1977) 519–542.
[2] F. Fahy, *Sound and Structural Vibration*, Academic Press, London, 1993.
[3] Š. Markuš, T. Nanasi, O. Šimková, Vibroacoustics of enclosed cavities, in: A.N. Guz (Ed.), *Dynamics of Bodies in Interaction with Surroundings*, Naukova Dumka, Kijev, 1991 (in Russian).
[4] J. Pretlove, Free Vibrations of a rectangular panel backed by a closed rectangular cavity, *Journal of Sound and Vibration* 2 (3) (1965) 197–209.
[5] J. Pan, D.A. Bies, The effect of fluid–structural coupling on sound waves in an enclosure-experimental part, *Journal of the Acoustical Society of America* 87 (2) (1990) 708–721.
[6] V.B. Bokil, U.S. Shirahatti, A technique for the modal analysis of sound–structure interaction problems, *Journal of Sound and Vibration* 173 (1) (1994) 23–41.
[7] C. Rajalingham, R.B. Bhat, G.D. Xistris, Vibration of circular membrane backed by cylindrical cavity, *International Journal of Mechanical Science* 40 (8) (1998) 723–734.
[8] M.-R. Lee, R. Singh, Analytical formulations for annular disk sound radiation using structural modes, *Journal of the Acoustical Society of America* 95 (6) (1994) 3311–3313.
[9] D.G. Gorman, J.M. Reese, J. Horáček, K. Dedouch, Vibration analysis of a circular disc backed by a cylindrical cavity, *Proceedings of the Institution of Mechanical Engineers, Part C* 215 (2001) 1303–1311.
[10] H.F. Bauer, M. Chiba, Hydroelastic viscous oscillations in a circular cylindrical container with an elastic cover, *Journal of Fluids and Structures* 14 (2000) 917–936.
[11] M. Amabili, G. Frosali, M.K. Kwak, Free vibrations of annular plates coupled with fluids, *Journal of Sound and Vibration* 191 (5) (1996) 825–846.

[12] M. Amabili, Effect of finite fluid depth on the hydroelastic vibrations of circular and annular plates, *Journal of Sound and Vibration* 193 (4) (1996) 909–925.
[13] A.W. Leissa, *Vibration of Plates*, NASA SP-160, Washington, 1969.
[14] N.W. McLachlan, *Bessel Functions for Engineers*, Oxford Engineering Science Series, Oxford University Press, London, 1948.
[15] C. Rajakumar, C.R. Rogers, The Lanczos algorithm applied to unsymmetric generalized eigenvalue problem, *International Journal for Numerical Methods in Engineering* 32 (1992) 1009–1026.